

## A ‘Maximum Entropy’-Based Novel Numerical Methodology for Problems in Statistical Electromagnetics

Kausik Chatterjee\*

**Abstract**—This paper presents the development of a novel ‘maximum entropy’-based numerical methodology for the solution of electromagnetic problems, where the inputs and system parameters vary statistically. The application of this methodology to the problem of a plane wave impinging on an array of cylindrical conducting rods with stochastic variations in its parameters is then presented. To address this problem, a statistically significant number of replicas of this array of conductors are constructed. The current profiles in these coupled conductors are estimated by using the Method of Moments (MoM). Upon estimation of the current profiles on the conductors, the monostatic radar cross-section is estimated for each replica of the array. The probability density function is then constructed through the estimation of a finite number of moments from the available output data subject to the constraint of maximum entropy. The methodology is very general in its scope and its application to scatterers with other geometries such as spheres, spheroids and ellipsoids as well as to other application areas would form the basis of our future work.

### 1. INTRODUCTION

In the recent years, with the advent of modern high speed computers, statistical electromagnetics [1–4] has gained significance and prominence as an area of cutting-edge research. In its essence, statistical electromagnetics involves the exploration of electromagnetic problems where the inputs as well as the system parameters can have statistical descriptions. The application areas are ubiquitous and range from the microscopic world of cell and tissue biology to the study of problems involving large antennas in the field of radio astronomy. For all of these problems, the use of numerical methods such as the Finite Difference Time Domain (FDTD) [5], the Finite Element (FEM) [6] or the Method of Moments (MoM) [7] leads to a matrix equation of the form  $\mathbf{L}\bar{y} = \bar{f}$ , where  $\bar{f}$  and  $\bar{y}$  are column vectors representing the input and the output respectively, while  $\mathbf{L}$  is a square matrix representing the system under consideration. In our problems of interest, both  $\mathbf{L}$  and  $\bar{f}$  can be defined stochastically and the challenge is to quantify  $\bar{y}$  or any function of  $\bar{y}$  in the stochastic sense.

### 2. UNCERTAINTY QUANTIFICATION: DETERMINISTIC AND STOCHASTIC

The quantification of uncertainty in input and system parameters can be deterministic or stochastic. In deterministic uncertainty quantification, numerical modeling is used to compute answers for the “entire” range of inputs and system parameters. Philosophically, it provides an exhaustive picture of the interaction. But it is also computer-intensive, particularly for problems where multiple quantities can have statistical variations. The need to solve multi-variable problems provides a rationale for developing statistical solution methodologies.

In statistical uncertainty quantification, one creates a statistically significant number of output samples by sampling the input and system variables and the solution methodologies fall in two broad categories:

---

*Received 30 May 2013, Accepted 3 January 2014, Scheduled 10 January 2014*

\* Corresponding author: Kausik Chatterjee (kausik.chatterjee@aggiemail.usu.edu and kausik.chatterjee.2@gmail.com).

The author is with the Space Dynamics Laboratory, Strategic and Military Space Division, Utah State University, North Logan, UT 84341, USA and also with the Center for Atmospheric and Space Sciences, Utah State University, Logan, UT 84322 USA.

- A. Polynomial Chaos (PC) Method [8–11]: In this method, orthogonal polynomials are used to decompose the output over the entire random space. Arguments of these polynomials follow known probability density functions. Accuracy and convergence rate depend on the choice of the PC system. Some commonly used PC systems are Legendre-Uniform, Hermite-Gauss and Laguerre-Gamma.
- B. Construction of Probability Density Function through Moments [12, 13]: In this method, a finite number of moments are estimated from the output data. The probability density function of the output is then estimated subject to a certain assumed criterion. One such criterion is the principle of “maximum entropy” [12, 13]. The requirement for a macroscopic physical system to reach the state of maximum entropy (a measure of disorder in the system) to achieve thermal equilibrium [14] is one of the most fundamental laws of statistical physics. In information theory, entropy is the measure of uncertainty in a random variable. The concept was introduced by Claude E. Shannon in his pioneering 1948 paper [15], “A Mathematical Theory of Communication”. Over the years, this principle has been used [12, 13] to estimate the probability density function of a random variable(s) from statistical data. The contribution of this paper is to apply this technique to problems in the area of statistical electromagnetics and this technique has the potential to be useful for problems that are current and important [2–4] in this area. In later sections of this paper, an entropy-based methodology will be developed for a classic scattering problem in computational electromagnetics.

### 3. PROBLEM OF INTEREST

The problem of interest involves a plane wave impinging on a symmetrical array of cylindrical conducting rods where the lengths and diameters of the conductors as well as the spacing between the conductors vary statistically and are assumed to follow Gaussian distributions. Our objective is to obtain a probability density function of the radar cross section (RCS) given the probabilistic nature of the parameters of the array.

With that goal in mind, a MoM-based formulation is constructed for the deterministic part of the problem. The formulation is an extension of the Pocklington’s integral equation [16–18] for a plane wave impinging on a single conductor. If the wire is very thin compared to the wavelength of the incident wave, the induced current can be approximated by an equivalent line current. An equivalent line current on the surface of the conductor along with observation points along the center of the conductor leads to the following integral equation [16]

$$\int_{-l/2}^{+l/2} I_z(z') \frac{e^{-j\beta R}}{4\pi R^5} \left[ (1 + j\beta R) (2R^2 - 3a^2) + (\beta a R)^2 \right] dz' = -j\omega\epsilon E_{z(\text{incident})} \text{ [Wire Center]}, \quad (1)$$

$$R = \sqrt{a^2 + (z - z')^2}, \quad \beta = \frac{2\pi}{\lambda},$$

where  $\lambda$  is the wavelength of the incident wave,  $l$  the length of the wire,  $a$  radius of the wire,  $R$  the distance between the induced current on the surface and observation point along the centerline, and  $E_z(z')$  the incident electric field. Above, the primed  $z$ -variable and unprimed  $z$ -variable refer to the coordinates of the induced line current on the surface and the coordinates of the observation points, respectively, and  $I_z(z')$  represents the induced line current on the surface. The geometry of the wire is shown in Fig. 1.

The current filament is divided into  $N$  segments. The use of  $N$  observation points along the center of the wire, leads to  $N$  linear equations. The approach easily generalizes to the coupled  $M$  conductor problem by calculating the effect of  $P = MN$  segments along the conductor boundaries at  $P$  observation points along the conductor centerlines, leading to a matrix equation where the unknowns are the currents in the  $P$  segments. A statistically significant number of ensembles is simulated based on the probability density functions of the system parameters and for each ensemble, the currents in the  $P$  line segments are estimated [16], which in turn are used to estimate the scattered electric field.

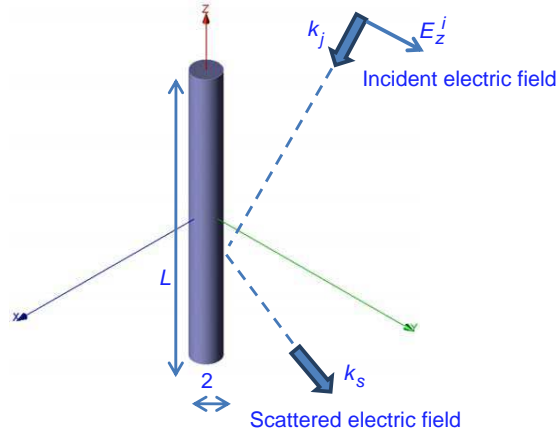


**Figure 1.** A plane wave impinging on a cylindrical wire.

The RCS of a three-dimensional object defined in terms of the electric field is given by

$$\sigma_{3-D} = \lim_{r \rightarrow \infty} 4\pi r^2 \frac{|\mathbf{E}_s|^2}{|\mathbf{E}_i|^2} \quad (2)$$

where  $\sigma_{3-D}$  is the RCS,  $r$  the distance from target to observation point,  $\mathbf{E}_s$  the scattered electric field, and  $\mathbf{E}_i$  the incident electric field. The probability density function of the RCS is then obtained using the principle of maximum entropy which is elaborated in the next section.

#### 4. PRINCIPLE OF MAXIMUM ENTROPY

The output space consists of a statistically significant number of  $(y_1, y_2, \dots, y_N)$  sample points and our goal is to estimate the probability density function,  $p(y)$  of the output. With that goal in mind, a finite number of moments of the output are estimated, where the  $n$ th moment is given by

$$m_n = \frac{\sum_{i=1}^N y_i^n}{N}, \quad n \geq 0. \quad (3)$$

The principle of maximum entropy involves maximizing the entropy function  $H[Y]$  given by

$$H[Y] = - \int_{-\infty}^{+\infty} p(y) \ln\{p(y)\} dy, \quad (4)$$

subject to constraints

$$\int_{-\infty}^{+\infty} y^n p(y) dy = m_n, \quad n \geq 0, \quad (5)$$

where the various moments are estimated from the obtained data. The constrained maximization of the entropy function is obtained using the well-known principle of Lagrange multipliers [12, 13] which is described in the next section. It should be noted that in Eq. (4),  $Y$  is a random variable that assumes values of  $y$  and follows a probability density function  $p(y)$ .

#### 5. PRINCIPLE OF LAGRANGE MULTIPLIERS

The objective is to maximize the function  $f(x, y)$  subject to the constraints  $g(x, y) = c$ . The principle of Lagrange multipliers introduces a Lagrange multiplier  $m$  and states that maximizing the unconstrained

Lagrange function  $L(x, y, m) = f(x, y) + m[g(x, y) - c]$ , meaning stipulating that the partial derivatives of  $L$  are zero, is equivalent to maximizing  $f(x, y)$  subject to the given constraints. As a result, the unconstrained expression  $H_u$  is maximized and is given by

$$H_u = - \int_{-\infty}^{+\infty} p(y) \ln p(y) dy - \sum_{n=0}^M \left( a_n \int_{-\infty}^{+\infty} y^n p(y) dy - m_n \right), \quad a_n \geq 0 \quad (6)$$

with respect to  $p(y)$ , where  $a_n$  are the Lagrange multipliers. Differentiating  $H_u$  with respect to  $p(y)$  and setting  $\partial H_u / \partial p(y) = 0$  leads to

$$\ln p(y) = -1 - \sum_{n=0}^M a_n y^n \quad (7)$$

$$p(y) = e^{-\left(1 + \sum_{n=0}^M a_n y^n\right)}. \quad (8)$$

Substituting  $p(y)$  from (8) in the constraint equations given by (5) gives rise to system of  $M+1$  nonlinear equations with  $M+1$  unknowns ( $a_0, a_1, \dots, a_M$ ), which in this work has been solved by an algorithm that uses the nonlinear conjugate gradient method [19]. In the next section, the results for the chosen benchmark problems are presented.

## 6. RESULTS

As mentioned in Section 3, the problem of interest involves a plane wave being incident on an array of conductors (Fig. 2), where the lengths and the diameters of the conductors as well as the spacing between the conductors vary statistically. The array of conductors is perpendicular and symmetrical about the  $x$ - $y$  plane. The polarization of the incident wave is in the  $+z$  direction and the direction of propagation is in the  $-x$  direction. As mentioned before, the output quantity of interest is the RCS defined in Section 3 (measured in the  $+x$  direction), and it is monostatic meaning the transmitter and the receiver share the same location. The MoM simulation is performed by converting the integral equation in (1) by using piece-wise constant sub-domain basis functions [16], where each conductor is divided into 8 segments. The details of the five benchmark problems are provided below:

1. A single conductor whose length varies according to Gaussian density function with mean equal to  $1/2$  of the wavelength and the standard deviation equal to  $1/10$  of the mean (Fig. 3).

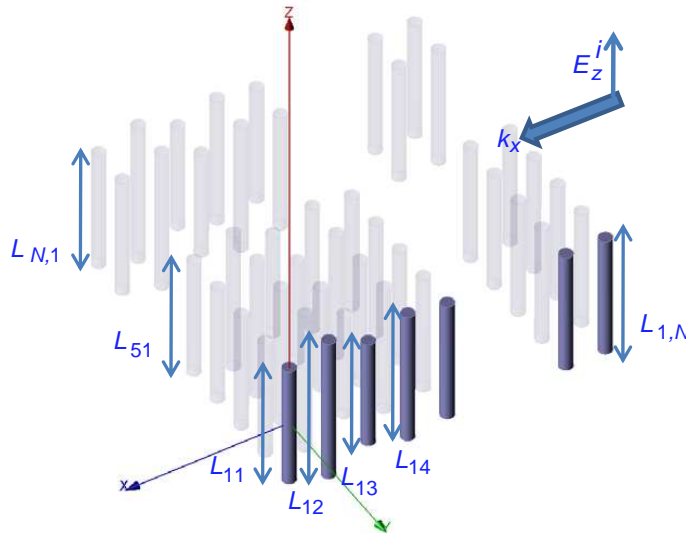


**Figure 2.** A plane wave impinging on a  $N \times N$  array.

2. A  $10 \times 10$  array where the lengths of the conductors vary according to the Gaussian density function given in Problem 1 (Fig. 4).
3. A single conductor whose length and diameter vary according to the Gaussian density function. The length of the conductor follows the distribution given in Problem 1. The mean diameter of the conductor is equal to  $1/10$  of the wavelength and standard deviation is equal to  $1/10$  of the mean (Fig. 5).
4. A  $10 \times 10$  array where the lengths and the diameters of the conductors vary according to the Gaussian probability density functions given in Problem 3 (Fig. 6).
5. A  $10 \times 10$  array where the lengths and the diameters of the conductors and also the spacing between the conductors follow the Gaussian probability density function. The lengths and the diameters of the conductor follow the distributions given in Problem 3. The mean spacing between the conductors is assumed to be  $1/2$  of the wavelength and the standard deviation is equal to  $1/10$  of the mean (Fig. 7).

In each of the five cases, the RCS data for 1000 ensembles have been gathered and 10 moments have been estimated to calculate the probability density function. The mean, variance, skewness and kurtosis for each of the five benchmark problems are shown in Table 1. The computation was performed on an UNIX-based platform with an Intel Xeon X5660 processor with a clock speed of 2.8 GHz and 32 GB

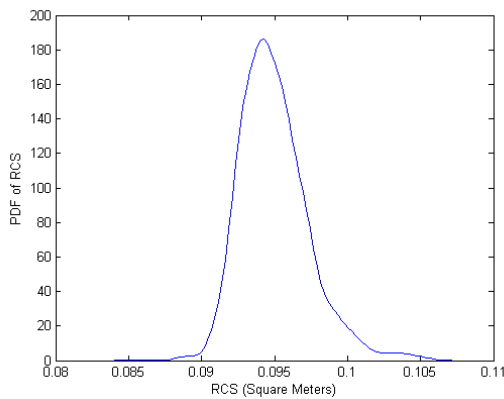


**Figure 3.** Probability density function for the radar cross section of a single conductor for Benchmark Problem 1.

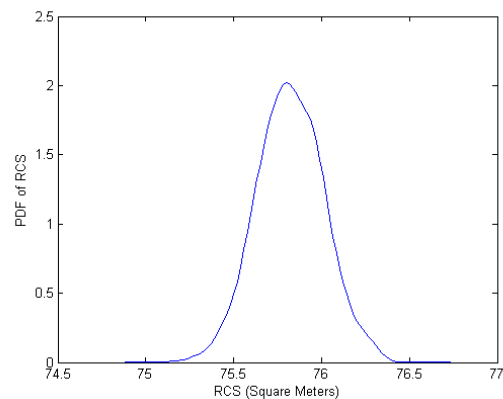


**Figure 4.** Probability density function for the radar cross section of an array of cylindrical conductors for Benchmark Problem 2.

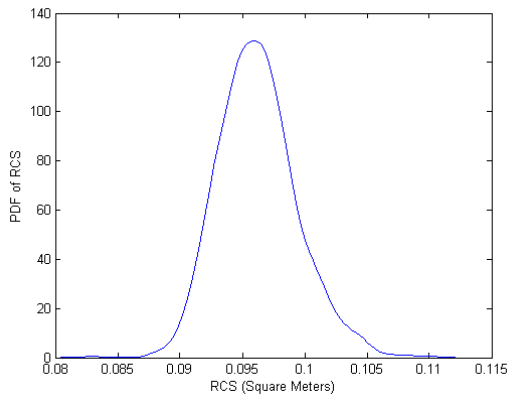


**Figure 5.** Probability density function for the radar cross section of a single conductor for Benchmark Problem 3.

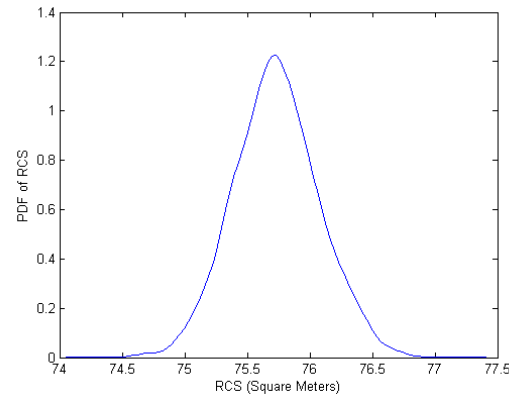


**Figure 6.** Probability density function for the radar cross section of an array of cylindrical conductors for Benchmark Problem 4.

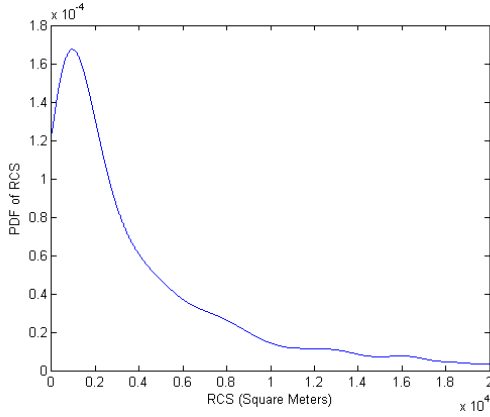


**Figure 7.** Probability density function for the radar cross section of an array of cylindrical conductors for Benchmark Problem 5.

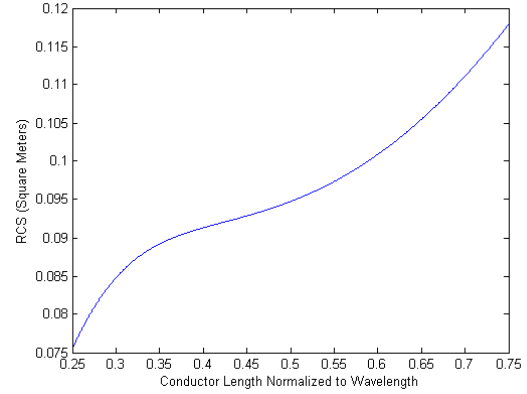


**Figure 8.** The radar cross section of a single conductor whose length changes deterministically between 5 standard deviations of the mean on either side.

**Table 1.**

Benchmark Prob.	Mean (m <sup>2</sup> )	Variance (m <sup>4</sup> )	Skewness (m <sup>6</sup> )	Kurtosis (m <sup>8</sup> )
1.	0.0950	$5.8595 \times 10^{-6}$	1.1826	6.1366
2.	75.8221	0.03541	-0.0139	2.9751
3.	0.0962	$1.0002 \times 10^{-5}$	0.4417	3.8345
4.	75.7301	0.1125	0.0488	3.0511
5.	$5.5470 \times 10^4$	$5.4945 \times 10^{11}$	26.4571	$7.6692 \times 10^2$

memory, while programming was performed using the C programming language. The computational times for the single conductor benchmark problems were of the order of the fraction of a second, while the computational times for the multi-conductor benchmark problems were of the order of a couple of minutes. The code was written to ignore negative values of conductor lengths and diameters, which were then resampled.

## 7. INTERPRETATION OF RESULTS

The five benchmark problems have been chosen keeping in mind the fact that the lengths, diameters and the spacing between different conductors are the only three parameters that can vary within an array. Within that, results have been provided for single conductors as well as for arrays. These parameters are assumed to follow Gaussian distributions keeping in mind real-life engineering applications. The mean length of the conductors and the spacing between the conductors are taken to be 1/2 of the wavelength of the incident wave, so that the problems are meaningful from an electromagnetic standpoint. On the other hand, the mean diameter of the conductors is taken to be 1/10 of the wavelength because the MoM formulation given in Section 3 is incumbent on the diameter being small compared to the incident wavelength. Based on the results obtained, the following inferences can be drawn:

1. Problems 1 and 3 are observed to have moderate positive skewness. This is because of the fact that even though the length and diameter of the single conductor follow Gaussian distributions with zero skewness, the induced current profile in the conductor and the resultant RCS is not linearly dependent on the length and the diameter. However, because of the coupling between conductors, the effect of having multiple conductors is to make the probability density function more symmetrical about the mean as evidenced by Problems 2 and 4. The enhanced symmetry results because the positive skewness introduced by one set of conductors is compensated by the negative

skewness introduced by the other set and with a statistically significant number of conductors and ensembles, a low value of skewness is obtained.

Problem 5 on the other hand results in a narrow probability density function with significantly larger skewness which can be attributed to the loss of regularity in the array and the resulting constructive and destructive interference between coupled scatterers with random phase differences. Then there are a few ensembles with very high RCS giving rise to a larger positive skewness as well as variance. Kurtosis measures how peaked a distribution is. Problems 1 to 4 exhibit moderate kurtosis which is to be expected because these problems show the effects of stochastically varying random variables that follow the Gaussian distribution with moderate kurtosis. Problem 5 on the other hand show very high kurtosis, which again can be attributed to the constructive and destructive interference between scatterers with random phase differences producing a narrow and peaked distribution.

In addition, by comparing Fig. 3 with Fig. 5 and Fig. 4 with Fig. 6, it is observed that the inclusion of an additional random variable leads to the lowering of the peak and the spreading of the distribution, as expected. For every one of the benchmark problems, it has been verified that the area under the curve is unity.

2. Benchmark Problem 1 involves a single conductor whose length varies stochastically. Now, the RCS of a conductor should increase with increasing length. As a result, the RCS for a conductor with a length of  $\mu - 5\sigma$  is  $0.0755 \text{ m}^2$ , the RCS for a conductor length of  $\mu$  is  $0.0947 \text{ m}^2$  and the RCS for a conductor length of  $\mu + 5\sigma$  is  $0.1179 \text{ m}^2$ , which matches the observations from Fig. 3. In Fig. 8, we present the RCS data for a single conductor whose length changes deterministically between five standard deviations of the mean on either side, where the monotonic nature of RCS variation is verified and the RCS values at the two extreme ends matches the values in the pdf plot (Fig. 3).
3. In Benchmark Problem 3, the RCS of a single conductor is studied, whose length and diameter vary stochastically. As a result, the RCS for a conductor whose length as well as diameter is  $\mu - 5\sigma$  equals  $0.0211 \text{ m}^2$ , the RCS for a conductor length whose length and diameter is  $\mu$  equals  $0.0947 \text{ m}^2$  and the RCS for a conductor whose length and diameter is  $\mu + 5\sigma$  equals  $0.1565 \text{ m}^2$ , which matches the observations from Fig. 5. It is to be noted that both the mean and diameter of the conductor being simultaneously  $5\sigma$  away from their respective means does not coincide with the  $5\sigma$  point of the output probability density function on either side of the mean.
4. If the conductors within the array were uncoupled the order of magnitude of the RCS of the array in Benchmark Problem 2 and Benchmark Problem 4 would have been approximately  $N^2$  times that of a single conductor,  $N$  being the array size. However, the mean RCS in Benchmark Problem 2 and Benchmark Problem 4 are seen to be one order of magnitude less than this estimate. This can be attributed to the fact that the currents in the conductors are strongly coupled. Of course, the geometrical factors do play a role, but that effect is a relatively smaller effect because the dimensions of the arrays are relatively small compared to the distance of the receiver from the array.
5. The comparison of results from Benchmark Problem 1 and Benchmark 3 show that the effect of stochastic variation in the diameter is relatively small. This can be attributed to the fact that the MoM formulation used is based on the assumption of diameter being small compared to the wavelength [16], while the mean length of the conductors is  $1/2$  of the wavelength.

## 8. CONCLUSION

In summary, a novel numerical methodology for the solution of electromagnetic problems has been developed where the inputs and system parameters have statistical descriptions. The novelty of the methodology lies in the use of the principle of maximum entropy to the solution of electromagnetic problems. The methodology has been successfully applied to the problem of a plane wave impinging on an array of cylindrical rods, where the lengths and diameters of the rods as well as the spacing between the rods vary statistically. A statistically significant number of ensembles of the array has been generated based on known probability density functions, and the probability density function of the RCS of the array has been constructed through the estimation of a finite number of moments and the use of

the principle of maximum entropy. It can be seen that same methodology can easily handle problems with multiple stochastically varying input and system parameters with the computational framework staying exactly the same. As a result, this entropy-based approach would be an attractive choice for a large class of problems without any restriction on the number of variables or the density functions these variables are allowed to follow. The RCS estimated in this paper is monostatic (meaning the transmitter and receiver at the same location), but it can easily be applied to the bistatic case, where the transmitter and the receiver are not at the same location. The extension of this approach to scatterers with other geometries such as spheres, spheroids and ellipsoids form the basis of our future work.

## ACKNOWLEDGMENT

This work was supported in part by the Air Force Office of Scientific Research through a grant (FA9550-06-1-0439) monitored by Dr. F. Fahroo. I acknowledge valuable discussions with Dr. Evgeny Mishin at Air Force Research Laboratory.

## REFERENCES

1. Holland, R. and R. S. John, *Statistical Electromagnetics*, Taylor & Francis, Philadelphia, PA, 1999.
2. Manfredi, P. and F. G. Canavero, "Impact of dielectric variability on modal signaling over cable bundles," *Proc. ESA Workshop on Aerospace EMC*, 1–4, Venice, Italy, May 2012.
3. De Menezes, L., D. Thomas, and C. Christopoulos, "Accounting for uncertainty in EMC studies," *Proc. EMC09*, 753–756, Kyoto, Japan, 2009.
4. Lallechere, S., S. Girard, P. Bonnet, and F. Paladian, "Enforcing experimentally stochastic techniques in uncertain electromagnetic environments," *Proc. ESA Workshop on Aerospace EMC*, 1–6, Venice, Italy, May 2012.
5. Taflov, A. and S. C. Hagness, *Computational Electromagnetics: The Finite-difference Time Domain Method*, 3rd edition, Artech House, Norwood, MA, 2005.
6. Hughes, T. J. R., *The Finite Element Method, Linear Static and Dynamic Finite Element Analysis*, Dover, Mineola, NY, 2000.
7. Harrington, R. F., *Field Computation by Moment Methods*, IEEE Press Series on Electromagnetic Wave Theory, Piscataway, NJ, 1993.
8. Xiu, D. and G. E. Karniadakis, "The Wiener-Askey polynomial chaos for stochastic differential equations," *SIAM J. Sci. Comput.*, Vol. 24, No. 2, 619–644, 2002.
9. Soize, C. and R. Ghanem, "Physical systems with random uncertainties: Chaos representations with arbitrary probability measure," *SIAM J. Sci. Comput.*, Vol. 26, No. 2, 395–410, 2005.
10. Stievano, I. S., P. Manfredi, and F. G. Canavero, "Parameter variability effects on multiconductor interconnects via hermite polynomial chaos," *IEEE Transactions on Components, Packaging and Manufacturing Technology*, Vol. 1, No. 8, 1234–1239, Aug. 2011.
11. Eldred, M., C. Webster, and P. Constantine, "Evaluation of non-intrusive approaches for Wiener-Askey generalized polynomial chaos," *49th AIAA/ASME/ASCE/AHS/ASC Structures, Structural Dynamics and Materials Conference*, Schaumburg, IL, Apr. 2008.
12. Papoulis, A. and S. U. Pillai, *Probability, Random Variable and Stochastic Processes*, 4th edition, 664–673, McGraw Hill, New York, NY, 2002.
13. Konrad, K., "Probability distributions and maximum entropy," Can be Accessed at the Website: [www.math.uconn.edu/~kconrad/blurbs/analysis/entropypost.pdf](http://www.math.uconn.edu/~kconrad/blurbs/analysis/entropypost.pdf).
14. Pathria, R. K., *Statistical Mechanics*, 2nd edition, Oxford, Butterworth Heinemann, 1999.
15. Shannon, C. E., "A mathematical theory of communication," *The Bell System Technical Journal*, Vol. 27, 379–423, Jul. 1948.
16. Balanis, C. A., *Advanced Engineering Electromagnetics*, 718–720, John Wiley & Sons, New York, 1989.

17. Miano, G., L. Verolino, and V. G. Vaccaro, "A new numerical treatment for Pocklington's integral equation," *IEEE Tran. on Mag.*, Vol. 32, No. 3, 918–921, May 1996.
18. Anders, R., "Minimum continuity requirements for basis functions used with the Pocklington integral equation," *Antennas and Propagation Society International Symposium*, Vol. 15, 284–287, Jun. 1977.
19. Nazareth, J. L., "Linear and nonlinear conjugate-gradient related methods," *Proc. App. Math.*, Vol. 85, Jan. 1996.